



OPEN ACCESS

EDITED BY

Magalie Viallon,
Centre Hospitalier Universitaire (CHU)
de Saint-Étienne, France

REVIEWED BY

Letizia Spinelli,
University of Naples Federico II, Italy
Kristopher Knott,
King's College Hospital NHS Foundation Trust,
United Kingdom

*CORRESPONDENCE

Kady Fischer
✉ kady.fischer@insel.ch

[†]These authors have contributed equally to this work and share first authorship

[†]These authors have contributed equally to this work and share senior authorship

RECEIVED 17 July 2023

ACCEPTED 05 September 2023

PUBLISHED 19 September 2023

CITATION

Weiner J, Heinisch C, Oeri S, Kujawski T, Szucs-Farkas Z, Zbinden R, Guensch DP and Fischer K (2023) Focal and diffuse myocardial fibrosis both contribute to regional hypoperfusion assessed by post-processing quantitative-perfusion MRI techniques. *Front. Cardiovasc. Med.* 10:1260156. doi: 10.3389/fcvm.2023.1260156

COPYRIGHT

© 2023 Weiner, Heinisch, Oeri, Kujawski, Szucs-Farkas, Zbinden, Guensch and Fischer. This is an open-access article distributed under the terms of the [Creative Commons Attribution License \(CC BY\)](https://creativecommons.org/licenses/by/4.0/). The use, distribution or reproduction in other forums is permitted, provided the original author(s) and the copyright owner(s) are credited and that the original publication in this journal is cited, in accordance with accepted academic practice. No use, distribution or reproduction is permitted which does not comply with these terms.

Focal and diffuse myocardial fibrosis both contribute to regional hypoperfusion assessed by post-processing quantitative-perfusion MRI techniques

Jeremy Weiner^{1†}, Corinna Heinisch^{1†}, Salome Oeri², Tomasz Kujawski¹, Zsolt Szucs-Farkas^{3,4}, Rainer Zbinden¹, Dominik P. Guensch^{2,4†} and Kady Fischer^{2*†}

¹Cardiology, Hospital Centre of Biel, Biel, Switzerland, ²Department of Anaesthesiology and Pain Medicine, Inselspital, Bern University Hospital, University of Bern, Bern, Switzerland, ³Radiology, Hospital Centre of Biel, Biel, Switzerland, ⁴Department of Diagnostic, Interventional and Paediatric Radiology, Inselspital, Bern University Hospital, University of Bern, Bern, Switzerland

Introduction: Indications for stress-cardiovascular magnetic resonance imaging (CMR) to assess myocardial ischemia and viability are growing. First pass perfusion and late gadolinium enhancement (LGE) have limited value in balanced ischemia and diffuse fibrosis. Quantitative perfusion (QP) to assess absolute pixelwise myocardial blood flow (MBF) and extracellular volume (ECV) as a measure of diffuse fibrosis can overcome these limitations. We investigated the use of post-processing techniques for quantifying both pixelwise MBF and diffuse fibrosis in patients with clinically indicated CMR stress exams. We then assessed if focal and diffuse myocardial fibrosis and other features quantified during the CMR exam explain individual MBF findings.

Methods: This prospective observational study enrolled 125 patients undergoing a clinically indicated stress-CMR scan. In addition to the clinical report, MBF during regadenoson-stress was quantified using a post-processing QP method and T1 maps were used to calculate ECV. Factors that were associated with poor MBF were investigated.

Results: Of the 109 patients included (66 ± 11 years, 32% female), global and regional perfusion was quantified by QP analysis in both the presence and absence of visual first pass perfusion deficits. Similarly, ECV analysis identified diffuse fibrosis in myocardium beyond segments with LGE. Multivariable analysis showed both LGE ($\beta = -0.191$, $p = 0.001$) and ECV ($\beta = -0.011$, $p < 0.001$) were independent predictors of reduced MBF. In patients without clinically defined first pass perfusion deficits, the microvascular risk-factors of age and wall thickness further contributed to poor MBF ($p < 0.001$).

Discussion: Quantitative analysis of MBF and diffuse fibrosis detected regional tissue abnormalities not identified by traditional visual assessment. Multi-parametric quantitative analysis may refine the work-up of the etiology of myocardial ischemia in patients referred for clinical CMR stress testing in the future and provide a deeper insight into ischemic heart disease.

KEYWORDS

quantitative perfusion, myocardial blood flow, fibrosis, stress-CMR, extracellular volume

Introduction

As ischemic heart disease remains one of the most common and fastest growing causes of mortality, the number of stress examinations to investigate inducible ischemia are rapidly expanding and are being performed in imaging centers outside of university hospitals. Cardiovascular magnetic resonance imaging (CMR) is considered one of the most comprehensive diagnostic imaging modalities and the advancement of parametric tissue characterization techniques allows for a deeper investigation into diffuse myocardial dysfunction.

A typical clinical CMR exam for ischemic testing relies mostly on a combination of qualitatively assessing myocardial perfusion under stress or a vasodilating stimulus and imaging of permanent myocardial injury or viability of the tissue (1). A comprehensive understanding of any underlying perfusion and tissue abnormalities can better risk stratify a patient with suspected coronary artery disease as both features have established incremental prognostic value to each other (2). Tissue viability is commonly assessed by late gadolinium enhancement (LGE). However, LGE is reliant on regional variability comparing enhanced myocardium to supposedly normal tissue and is ideal for investigating replacement scar associated with infarct, but it can consequently overlook diffuse fibrosis. Calculation of extracellular volume (ECV) through parametric T1 maps can overcome this limitation to non-invasively depict the fibrotic burden per voxel (3). Similarly, the routine clinical analysis of myocardial perfusion commonly includes qualitative first pass perfusion (FPP) analysis, where delays in the arrival of contrast agent to the myocardium are visually assessed and classified as a perfusion deficit. FPP also performs poorly in balanced ischemia in three-vessel disease or microvascular dysfunction because of diffusely decreased contrast agent uptake in all or most segments (4), and detection of perfusion deficits relies heavily on the experience of the examiner (5). As a result, there is increased interest into development of quantitative perfusion (QP) techniques. With a fully quantitative analysis, absolute myocardial blood flow (MBF) is assessed for each pixel and expressed in milliliters per gram of myocardial tissue per minute (ml/g/min) (6) thereby it is not reliant on visual appreciation of regional differences. In comparison to T1 and ECV mapping, QP is not yet as established and its implementation is limited. There are a variety of QP techniques available, with many publications using novel sequences with inline MBF analysis. However, access to these specialized sequences may not be as widely available outside of tertiary research centers. An alternative to increase access to QP could be to apply post-processing software techniques that quantify MBF from product first pass perfusion sequences (7–10).

Thus, we investigated the use of post-processing techniques for quantifying pixelwise MBF in comparison to standard clinical visual analysis of visual FPP in patients undergoing clinically indicated CMR stress testing. Moreover, to shed light on potential discrepancies in regional and global hypoperfusion between the two perfusion analysis techniques we investigated if

patient characteristics and quantification of other myocardial features acquired within the same multi-parametric CMR could explain MBF findings acquired by QP post-processing analysis. In particular, the primary aim was to investigate if visually assessed focal scar and quantified diffuse fibrosis have an independent impact on QP-derived MBF under regadenoson stress.

Methods

Study design & patient enrolment

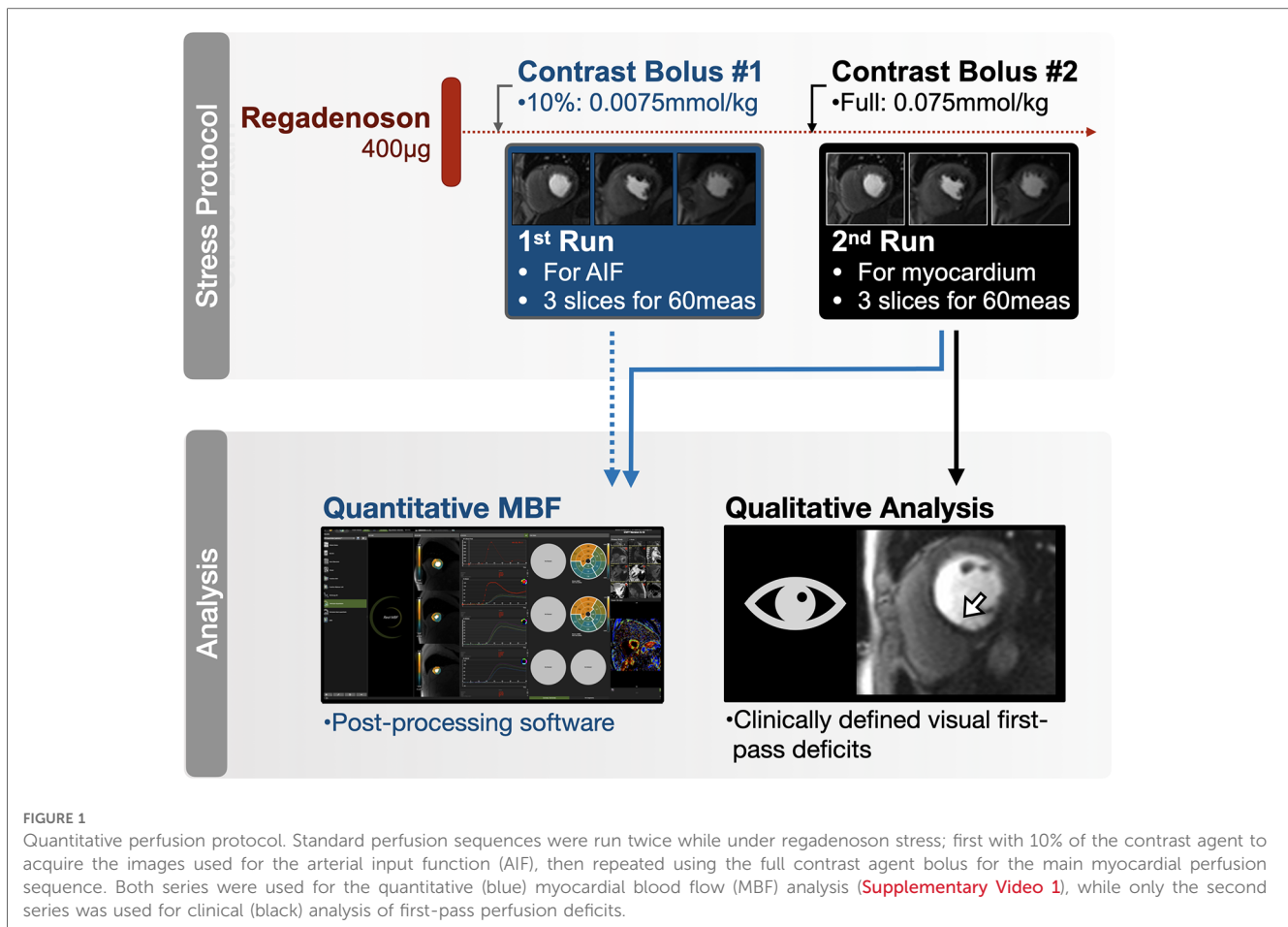
The study was approved by the ethics board of the Canton of Bern, Switzerland (2021_00139) and complies with the Declaration of Helsinki. All subjects had given their written informed consent before enrolment into this study. This was a prospective observational study that enrolled 125 patients at the Hospital Centre of Biel, Switzerland who were referred for a clinically indicated stress-CMR to investigate inducible ischemia (May 2021–May 2022). Exclusion criteria were caffeine consumption in the last 12 h, <18 years of age, inability to give consent, or patients deemed unfit for an extended protocol by the imaging physician.

CMR exam

The CMR studies were performed using a clinical 1.5 T MRI (Magnetom Sola, Siemens Healthineers). Patients underwent cine imaging with a short axis stack and three long-axis views for functional analysis. Stress was induced with intravenous administration of regadenoson (fixed dose of 400 µg), and perfusion at stress was imaged using a dual bolus protocol (10, 11) (Figure 1). FPP images were acquired with a standard product gradient echo-based pulse sequence in three short-axis slices, initially using a 10% bolus of contrast agent required for QP (0.0075 mmol/kg, Gadovist, Bayer) for determining the arterial input function (AIF). The sequence was then repeated with the full contrast agent dose (0.075 mmol/kg). After stress the remaining contrast agent was given to reach a total dose of 0.15 mmol/kg, and LGE images were acquired for the assessment of focal scar eight minutes after the third bolus. T1 maps in three short-axis slices were acquired prior to and after contrast agent injection for the calculation of ECV as a measure of diffuse fibrosis. Sequence details are provided in the [Supplementary Methods](#).

CMR image analysis

Images were analyzed by three independent groups of readers. First, a clinical analysis was performed by the local imaging team of senior physicians with CMR certification and >5 years of CMR experience. The clinical report included volumetric function, septal wall thickness and a visual assessment of the presence of



LGE and qualitative FPP deficits. The presence or absence of the latter two parameters were reported for each myocardial segment [American Heart Association (AHA) 16-segment model] and classified by distribution pattern. A semiquantitative segment score was calculated for both measures based on the sum of segments with either LGE enhancement or visual FPP deficits. A patient was reported to have clinically relevant inducible ischemia by the presence of two adjacent segments with visual FPP deficits and have clinically relevant LGE if any myocardial enhancement was detected.

For quantitative analysis performed for research purposes, images were then recoded. Then QP and T1 maps were each analyzed by blinded readers, who did not take part in the first reading session. QP and T1 maps were both analyzed using CVI⁴² (Circle Cardiovascular Imaging, version 5.13). For the quantitative perfusion contours were added automatically and adjusted by the reader if required. Hyperemic myocardial blood flow (MBF) per voxel was then quantified by the software and reported as numerical result per AHA segment and for a global MBF (8, 10). Pixel-wise MBF maps were also generated and used for the correction of contours (Supplementary Video 1). Ten datasets were randomly selected and reanalyzed for a blinded intra- and interobserver assessment each. Pre- and post-contrast T1 maps were analyzed for myocardial and blood pool signal and ECV was calculated and reported as percent

(12). For categorical comparisons ECV was dichotomized by a cutoff of 30%.

Statistical analysis

Patients were included in the final analysis if QP, ECV and LGE were all successfully acquired. For the primary endpoint, the relationship between other CMR findings and patient characteristics to global and segmental MBF were assessed with a univariable linear regression. Continuous variables were utilized for MRI measurements such as segment score for LGE and visual FPP, or % for ECV. Significant variables ($p < 0.05$) were then forwarded into a multivariable model. For secondary analysis investigating categorical comparisons, global and segmental MBF from QP analysis were grouped based on the presence of LGE and $ECV \geq 30\%$ and compared with a multivariate ANOVA and Tukey's *post-hoc* tests accounting for multiple comparisons. Similar models were used to compare the visual and quantitative techniques. Quantified MBF (ml/g/min) was compared between segments categorized by the presence and distribution of visual FPP deficits. The same analysis was performed for ECV(%) in the presence of LGE. For tests using segmental analysis, multiple measures per patient were accounted for in the statistical models. Intra- and interobserver reliability

was calculated with an intra-class correlation (ICC) test for absolute agreement. Results were considered statistically significant at a two-tailed value $p < 0.05$. Statistical analyses were performed with GraphPad Prism version 9.0 (GraphPad Software) and R software (version 3.5.0, R Foundation for Statistical Computing).

Results

Patient characteristics and inclusion

From the 125 patients prospectively enrolled (Table 1), 109 were included in the final analysis (87%). In eight (6%) patients either the AIF pre-bolus sequence or T1 maps were not acquired, in five (4%) patients it was decided during the CMR to not give pharmacological stress, and in three (2%) patients, there was an error with the software and QP could not be calculated

TABLE 1 Patient characteristics.

| | Total (n = 109) |
|--|-----------------|
| Age, years | 66.5 ± 10.9 |
| Sex (females) | 34 (32%) |
| Body mass index, kg/m ² | 28 ± 5.2 |
| Indication for stress-CMR | |
| Stable angina pectoris/ECG abnormalities | 51 (47%) |
| Dyspnea/exercise intolerance of unclear origin | 17 (16%) |
| Suspected ischemia secondary to other disease | 15 (14%) |
| Follow-up of known CAD | 13 (12%) |
| Echocardiography abnormalities | 7 (6%) |
| Other | 6 (5%) |
| Comorbidities | |
| Hypertension | 63 (58%) |
| Dyslipidemia | 56 (51%) |
| Diabetes mellitus | 29 (27%) |
| Sleep apnea syndrome | 16 (15%) |
| History of CAD | |
| Myocardial infarction | 18 (17%) |
| Coronary intervention | 31 (28%) |
| Atrial fibrillation | 12 (11%) |
| Obesity | 25 (23%) |
| Infiltrative diseases | 0 (0%) |
| Medication | |
| Anti-platelets | 36 (33%) |
| Dual anti-platelets | 9 (8%) |
| Anti-coagulants | 19 (17%) |
| ACE inhibitors | 28 (26%) |
| Angiotensin II receptor blockers | 36 (33%) |
| ARNI | 2 (2%) |
| Calcium channel blockers | 22 (20%) |
| Spironolactone | 4 (4%) |
| SGLT-2 inhibitors | 9 (8%) |
| Beta-blockers | 44 (40%) |
| Diuretics | 31 (28%) |
| Anti-lipid therapy | 55 (50%) |

Mean ± standard deviation, or frequency (percentage) are shown. ACE, angiotensin-converting-enzyme; ARNI, angiotensin receptor neprilysin inhibitor; CAD, coronary artery disease; ECG, electrocardiogram; SGLT-2, sodium-glucose cotransporter-2.

(Supplementary Figure S1). Patient characteristics are provided in Table 1, mean age was 66.5 ± 10.9 years, 34% were females. Hypertension (58%) and dyslipidemia (51%) were the most common comorbidities. Left ventricular ejection fraction was 60.1 ± 12.7%, cardiac output of 5.9 ± 2.2 L/min and a septal wall thickness of 10.8 ± 2.7 mm.

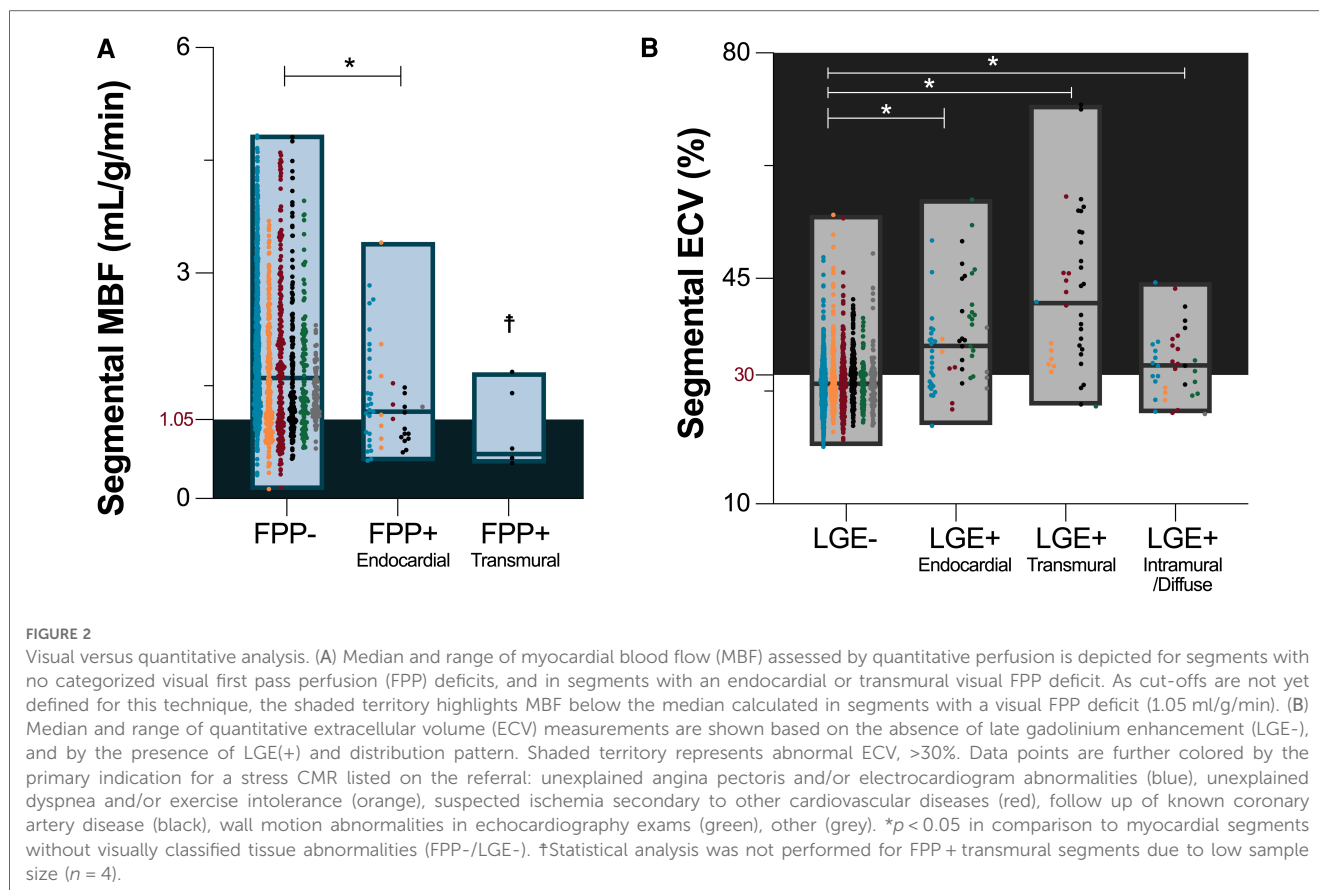
Comparison of visual and quantitative analysis

All included patients presented with signs of a sufficient hemodynamic response during regadenoson, defined by an increase in heart rate of ≥10 bpm (18 ± 7 bpm) and/or a drop in systolic blood pressure of ≤−10 mmHg [−5.0 (−16–2.5)mmHg]. Of the 109 patients, 22 (20%) had a visually classified FPP deficit in at least one myocardial segment, and 10 patients (9%), were diagnosed with a clinically relevant inducible ischemia, defined by adjacent segments with FPP deficits. Regionally, the majority of segments with a visual FPP deficit were classified with endocardial hypoperfusion ($n = 50$), while the remainder had transmural hypoperfusion ($n = 4$). MBF was higher in segments without visual FPP deficit [1.6 (1.1–2.3 ml/g/min)], than those with a classified FPP deficit [1.2 (0.8–1.6)ml/g/min, $p < 0.001$]. Yet as shown in Figure 2, the range of MBF in visually classified normal segments was large with a clear overlap between segments with FPP deficits.

For the assessment of fibrosis, LGE was present in 41(38%) patients. In these patients presenting with LGE, enhancement was observed in a median of 3 [1–5] AHA segments (/16). Of the 132 total segments with LGE, 63 were classified with a sub-endocardial distribution, 40 as transmural and 29 as intramural/diffuse. Quantitative analysis of ECV as a pixelwise measurements of diffuse fibrosis was lower in segments without LGE than with LGE [28.6 (26.2–31.0)% vs. 34.7 (30.5–40.9)%, $p < 0.001$]. This trend was significant, independent if the LGE distribution was sub-endocardial, transmural or intramural/diffuse (Figure 2). Similar to MBF and visual FPP analysis, the range of ECV in segments without LGE was large, and a portion of these segments (36%) were above the cutoff of 30% indicating these patients had fibrosis that was only detected by quantitative measurements and not the traditional LGE technique.

Factors impacting global myocardial blood flow

Median global MBF from the QP analysis was 1.6 (1.2–4.1)ml/g/min. Twenty-five (23%) patients presented positive for both LGE and ECV ≥30% averaged across the whole heart (LGE+/ECV+), 22 (20%) patients had elevated ECV but no LGE (LGE-/ECV+), 16 (15%) patients had LGE with ECV <30%, and 46 (42%) patients presented with no LGE or ECV elevation (Figure 3A). Global MBF during stress was lowest [1.2 (1.0–1.8) ml/g/min] in patients that presented with both a globally elevated ECV and LGE in comparison to all other categories ($p < 0.05$ vs. all).



However, there was no difference between the other three categories, even if there was either LGE or ECV abnormalities [LGE-/ECV+: 1.7 (1.2–2.6), LGE+/ECV-: 2.2 (1.7–2.7), LGE-/ECV-: 1.6 (1.3–2.3) ml/g/min]. Univariable analysis investigating variables that impact MBF demonstrated that increased age, males, low ejection fraction and cardiac output, increased wall thickness, ECV(%) and number of segments with LGE all had significant associations ($p < 0.05$, all β - coefficients provided in **Supplementary Table 1**). In the multivariable analysis none of these factors were independently linked to global MBF (**Figure 4**).

Factors impacting segmental myocardial blood flow

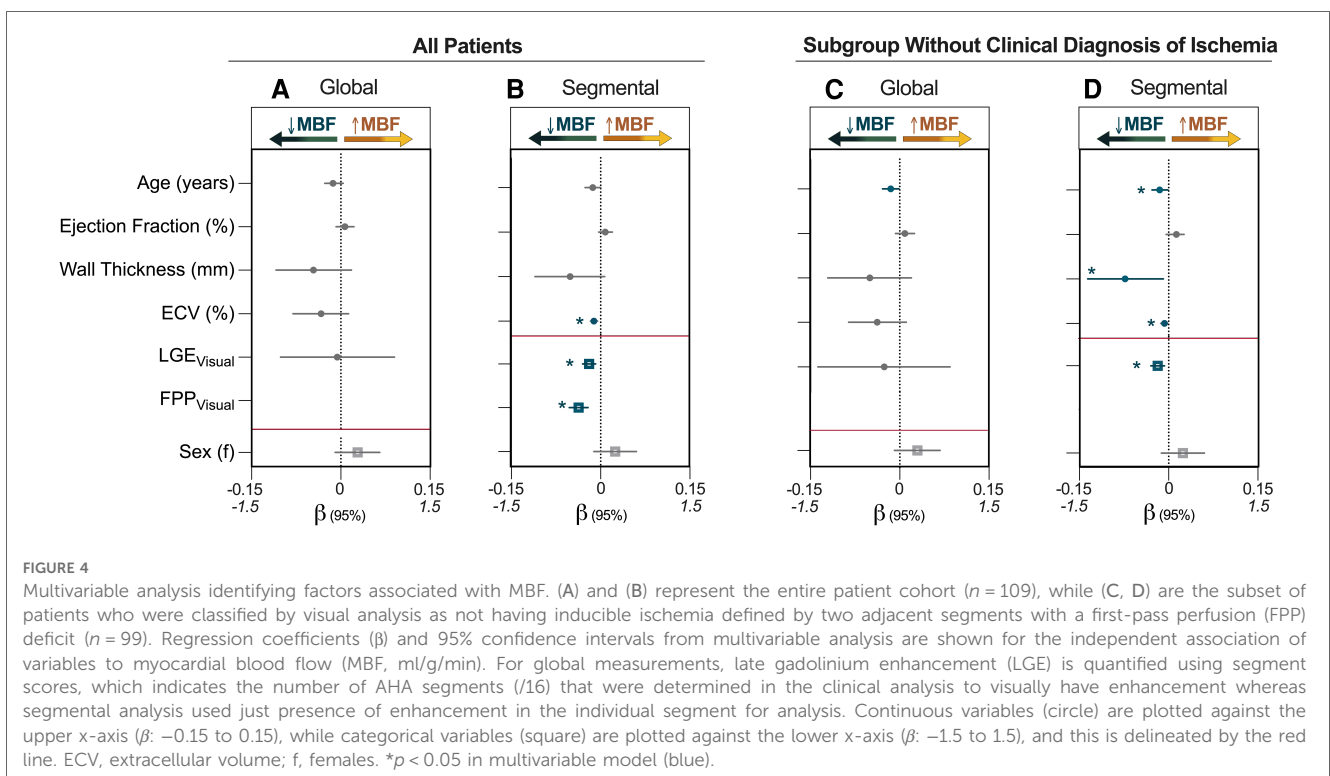
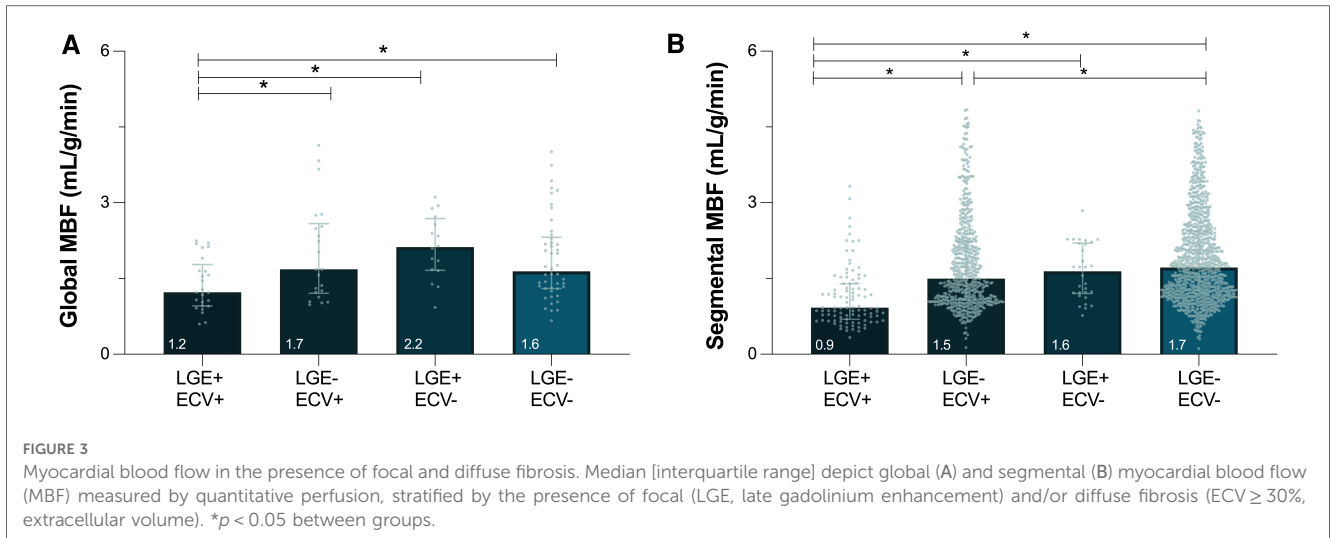
When investigating individual segments ($n = 1,695$), 6% had both LGE and $ECV \geq 30\%$ (LGE+/ECV+), 35% of the segments had $ECV \geq 30\%$ but no LGE (LGE-/ECV+), only 2% of segments showed LGE with $ECV < 30\%$, and 57% patients presented with no LGE or ECV elevation. Similar to global analysis, segments presenting with both LGE and $ECV \geq 30\%$ had a MBF of 0.9 [0.6–1.4]ml/g/min, which was significantly lower than the three other categories ($p < 0.05$ vs. all). Moreover, even in the absence of LGE, segments with $ECV \geq 30\%$ yielded lower MBF than segments without diffuse fibrosis [LGE-/ECV+: 1.5 (1.1–2.2)ml/g/min vs. LGE-/ECV-: 1.7 (1.2–2.4)ml/g/min, $p = 0.041$], whereas

the few segments with LGE+/ECV- did not differ [1.6 (1.2–2.2) ml/g/min, $p = 0.329$].

Univariable segmental associations are provided in **Supplementary Table 2**. In the multivariable analysis, the presence of a visual perfusion deficit ($\beta = -0.370$, $p < 0.001$), LGE ($\beta = -0.191$, $p = 0.001$) and ECV ($\beta = -0.011$, $p < 0.001$) all independently explained the MBF accounting for multiple measurements per subject. Taking this one step further, univariable and multivariable analysis was again performed for the subset of patients ($n = 99$) that did not have clinical classification of inducible ischemia (two or more adjacent segments with an FPP deficit). In these patients, presence of LGE ($\beta = -0.183$, $p = 0.002$) and elevated ECV ($\beta = -0.007$, $p = 0.035$) still independently explained a lower segmental MBF, but in this subgroup increased age ($\beta = -0.015$, $p = 0.040$) and a larger wall thickness ($\beta = -0.073$, $p = 0.030$) were also independently associated with MBF (**Figures 4, 5, Supplementary Table 3**).

Reader reliability of QP

Reader reliability (**Figure 6**) for the QP measurements was excellent for intraobserver [ICC = 0.99 (0.98–0.99), $p < 0.001$] and interobserver [ICC = 0.98 (0.94–0.99), $p < 0.001$] global MBF quantification. Similar reliability was yielded for segmental MBF quantification [intraobserver: ICC = 0.98 (0.98–0.99), $p < 0.001$, interobserver: ICC = 0.96 (0.94–0.97), $p < 0.001$].



Discussion

In a cohort of patients undergoing clinical stress CMR exams, analysis of pixel-wise MBF by post-processing quantitative perfusion (QP) software was feasible, reliable and was successfully performed in 97% of the acquired exams with pharmacological vasodilation. Hypoperfusion was identified in patients undergoing stress CMR, in both the presence and absence of visually assessed first pass perfusion (FPP) deficits. Even in patients who were not diagnosed with inducible ischemia by visual FPP analysis, both the presence of focal and diffuse fibrosis represented

by the presence of LGE and ECV along with a thicker septal wall and patient age were independently associated with reduced regional MBF.

Pixelwise quantitative analysis

In this study, both traditional qualitative and modern quantitative analysis techniques were applied to characterize the myocardial tissue features of perfusion and fibrosis. In the case of diffuse perfusion abnormalities and fibrosis patterns, abnormalities can remain undetected with the

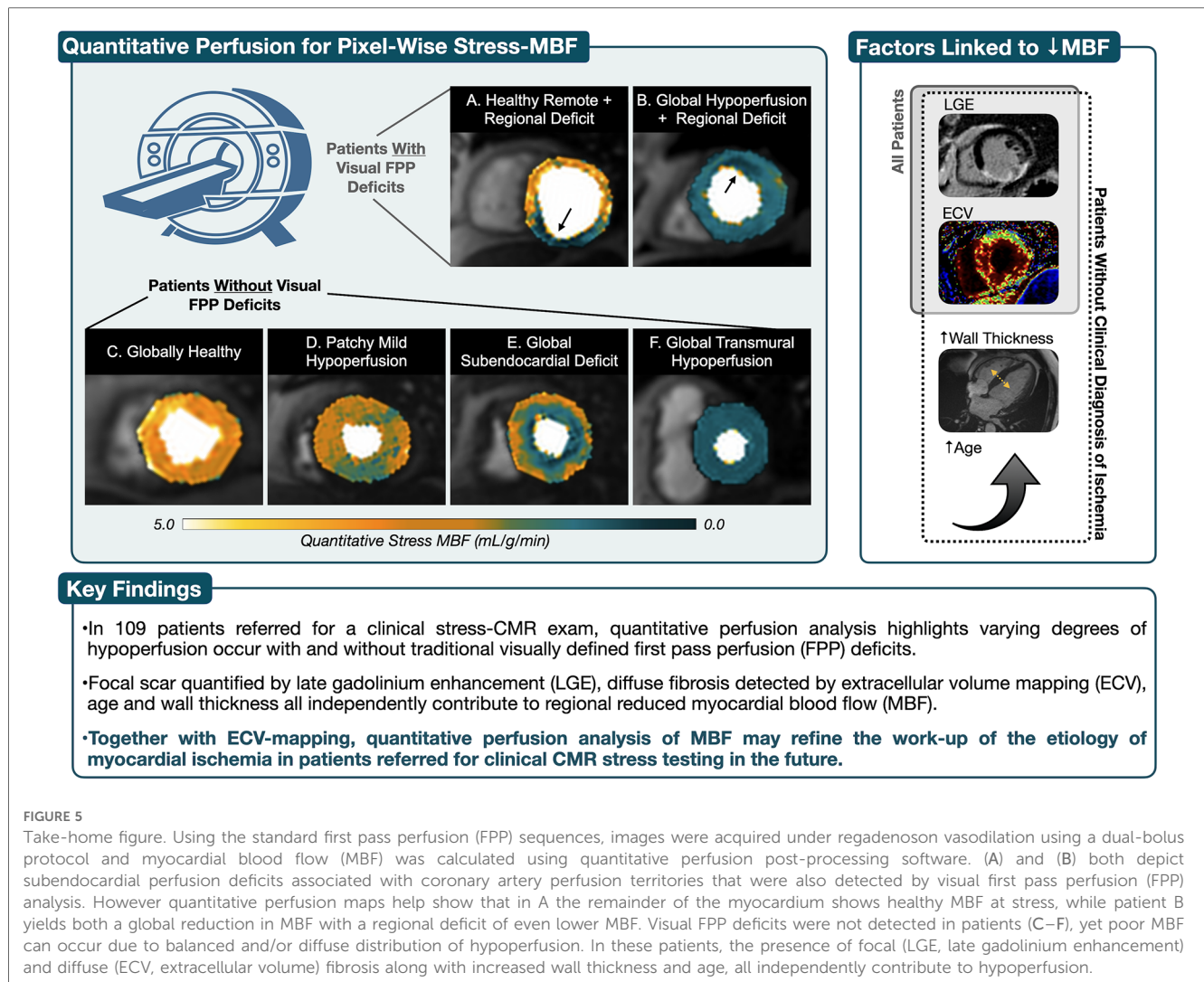


FIGURE 5

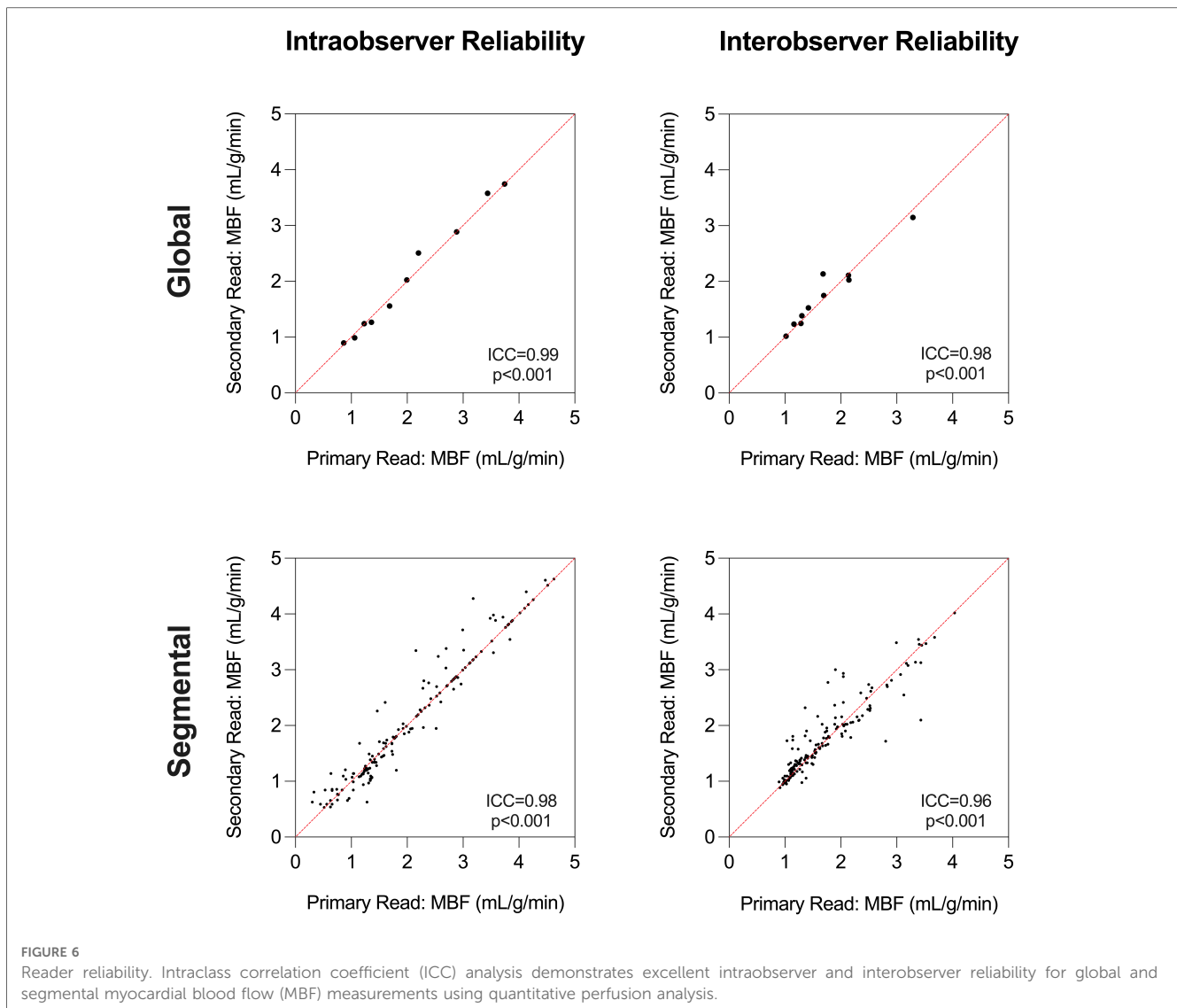
Take-home figure. Using the standard first pass perfusion (FPP) sequences, images were acquired under regadenoson vasodilation using a dual-bolus protocol and myocardial blood flow (MBF) was calculated using quantitative perfusion post-processing software. (A) and (B) both depict subendocardial perfusion deficits associated with coronary artery perfusion territories that were also detected by visual first pass perfusion (FPP) analysis. However quantitative perfusion maps help show that in A the remainder of the myocardium shows healthy MBF at stress, while patient B yields both a global reduction in MBF with a regional deficit of even lower MBF. Visual FPP deficits were not detected in patients (C–F), yet poor MBF can occur due to balanced and/or diffuse distribution of hypoperfusion. In these patients, the presence of focal (LGE, late gadolinium enhancement) and diffuse (ECV, extracellular volume) fibrosis along with increased wall thickness and age, all independently contribute to hypoperfusion.

qualitative approaches because of the absence of healthy reference myocardium. This regional analysis technique can be compromised in the case of balanced impaired perfusion, arising from pathological processes including microvascular disease or 3-vessel CAD (4, 13). This could explain why only a portion of our patients received a clinical diagnosis of inducible ischemia from FPP analysis, despite suspicion of myocardial ischemia leading to the referral for a stress-CMR, and low MBF yielded from QP analysis. Similarly, others have shown visual FPP analysis underestimates the ischemic burden in multivessel disease, and quantitative perfusion was better at identifying the extent of two- and three-vessel disease CAD (13). QP isn't limited to highlighting balanced hypoperfusion but it can help clarify regional variation. For example in **Figure 5**, both panels A and B have a regional deficit visualized by FPP, yet in patient A the remainder of the myocardium has normal MBF with a small region of hypoperfusion, while in patient B, the entire myocardium is compromised with very low MBF in the anterior wall. These differences are patterns that cannot be distinguished by qualitative FPP analysis.

Factors associated with decreased segmental MBF

Our results demonstrate the importance of segmental analysis. Averaging the entire myocardium into a single global MBF can lead to false negative results, if a regional perfusion deficit or a focal elevated ECV is compensated for or cancelled out by an otherwise healthy myocardium, resulting in a normal global value. Similarly, it was reported in hypertrophic cardiomyopathy patients that comparison of global MBF did not differ between patients with and without visual perfusion deficits, but investigation of individual segments revealed significant insights into regional decrease in perfusion (14). Thus, segmental analysis is beneficial to verify hypoperfusion, and to co-localize associated myocardial features (15–17).

In this cohort, as expected, the presence of a visual perfusion deficit and LGE were both associated with a co-localized segmental reduction in MBF. Hypoperfusion and tissue-injury have a mutually antagonistic relationship with each other. While poor blood flow can lead to myocardial ischemia and development of myocardial edema and fibrosis, structural damage to the tissue itself also impedes myocardial blood flow

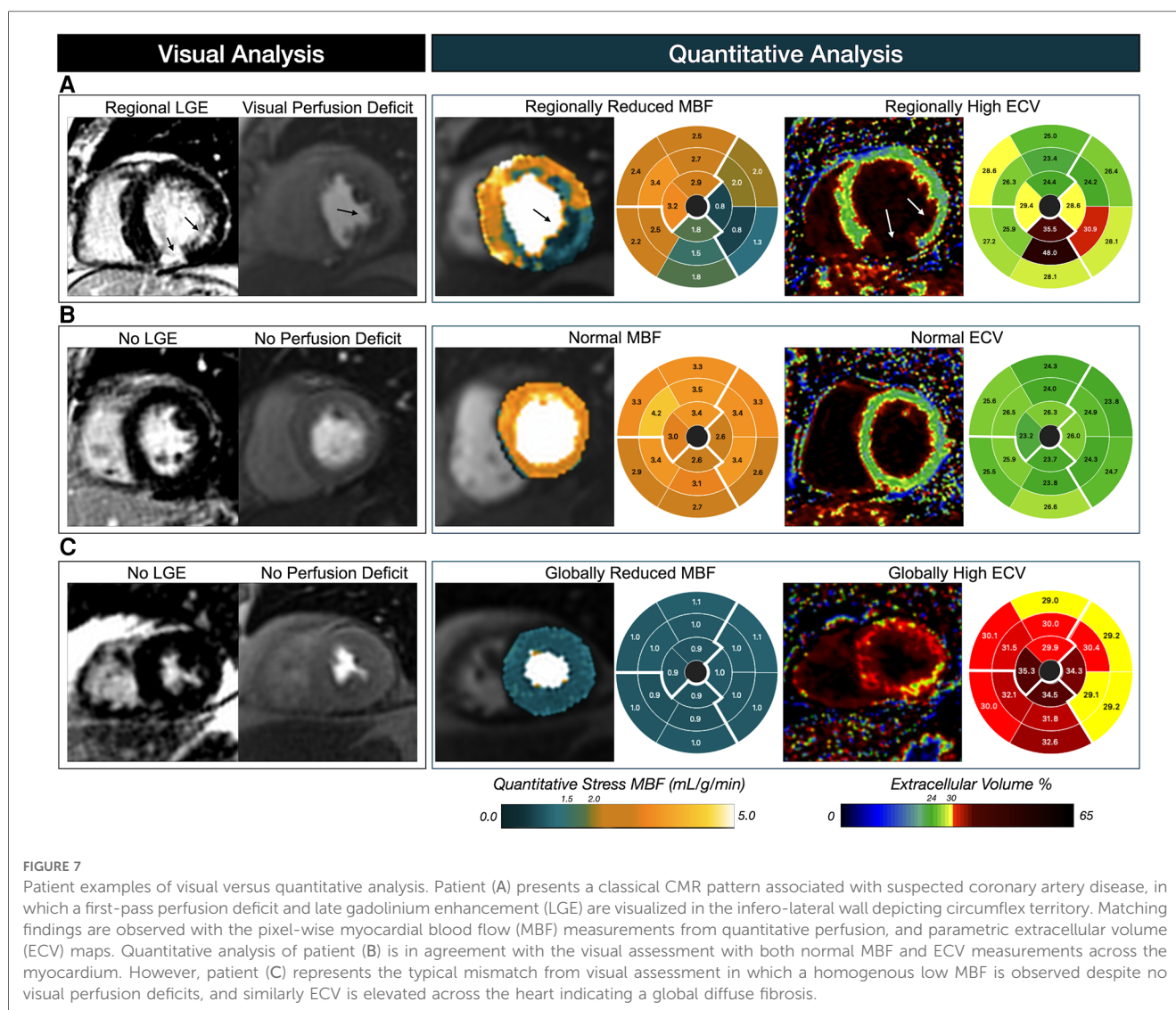


which subsequently can lead to further tissue injury (18). LGE excels at viability analysis and depicting replacement scar associated with myocardial infarction. Infarct scar is typically brought about by ischemic insults, in which myocytes are lost through necrosis and replaced by fibrotic scar. On the other hand, diffuse fibrosis often results as a reactive process of increased collagen deposition among myocytes, with typically less myocyte degradation (19). Consequently, LGE has lower accuracy in identifying these diffuse alterations in the myocardium (20). Diffuse fibrosis can impact the microvasculature and perfusion reserve through multiple mechanisms including stiffening of the ventricles leading to increased filling and intramural pressures, an increase in intercellular space and consequent change in microvascular architecture (21–23). Especially in the absence of infarct and obstructive macrovascular disease diffuse fibrosis can play a significant role in the microvascular dysfunction and microischemia (24, 25).

The fact the perfusion is attenuated in the presence of fibrosis is well established (26), but the difficulty had been that it was not

manageable to routinely visualize and include measures of diffuse hypoperfusion and fibrosis into clinical reporting. The new aspect of this investigation is that we demonstrate that through post-processing methods, the hypoperfusion observed with QP and not FPP is influenced independently by both the traditional clinical LGE analysis and by the quantification of diffuse fibrosis. While ECV can depict the infarct core highlighted by LGE as seen in **Figure 7**, the parametric nature of this marker allows it to quantify additional myocardial abnormalities beyond the classical infarct-related scar (27). It should be noted, that ECV is not specific to myocardial fibrosis, but can also be seen with other myocardial injury as T1 and ECV maps can also depict edema and hemorrhage (3, 28–30).

We also observed in the sub-analysis that other factors beyond replacement and diffuse forms of myocardial fibrosis impact MBF. Increased age and larger wall thickness, both considered risk-factors for microvascular dysfunction, were also independently associated with reduced MBF. Measures of fibrosis along with increased wall thickness has already been linked to poor vascular



function in specific pathological settings as in hypertrophic cardiomyopathy, Anderson-Fabry disease and HFpEF (31–33). Consequently, especially in patients who do not present with the typical ischemia pattern detected by FPP, i.e., subendocardial hypoperfusion localized to the center of one or two perfusion territories, hypoperfusion should not be discounted if these other imaging features associated with microvascular disease and global ischemia are present.

Moving towards quantitative clinical analysis

QP has been primarily reserved to research settings, but multiple directions are currently developing techniques to translate QP to clinical routine such as through generation of in-line automated perfusion maps with respiratory motion correction, or through off-line software (4, 9, 34). Used for a clinical purpose, QP would potentially offer a more objective evaluation of ischemia and hypoperfusion.

This study uses a dual-bolus technique instead of the more validated dual-pulse single-bolus approach, where both the AIF and myocardial stress are acquired within the same acquisition. The main disadvantages of the applied dual-bolus technique is that it can be prone to T2* effects, it requires longer imaging time under stress as the sequence has to be repeated individually for the AIF and myocardial stress, and inline maps are not provided on the scanner (4, 35). However, a key advantage is that our approach does not require specialized sequences that may not be widely available outside of university hospitals. Rather we used the standard product sequence already implemented into our clinical routine and we were able to quantify MBF post-hoc with software without interfering with the traditional FPP images, which many clinicians still currently rely on for clinical decision making. For the current time, this technique presents a bridging option for imaging sites at secondary hospital or diagnostic centers which do not have access to developing sequences.

This combination of a dual-bolus protocol and post-processing software we have applied in our analysis was recently validated to fractional flow reserve measurements by Zhao et al. (10).

Nevertheless, further comparisons between the approaches are needed in the future, especially for detection of microvascular dysfunction. So far in research settings, optimal cut-offs ranging from 1.2–2.6 ml/g/min have been reported to identify and risk stratify CAD patients, yet these come from different approaches and pharmacological agents resulting in a wide range of normal values (4, 8, 10, 34, 36, 37). In our cohort, global median MBF was 1.6 ml/g/min with a lower and upper interquartile range of 1.2–4.1 ml/g/min respectively. Regional median MBF dropped to about 1.2 ml/g/min in segments with a FPP deficit and/or LGE+/ECV+ segments, while a median of 2.2 ml/g/min was observed in segments with no fibrosis. These medians are in the lower range of reported MBF, especially in comparison to reports using adenosine (4, 10). While there is also variation in MBF among studies using regadenoson (8, 37, 38), independent studies have reported MBF similar to ours while using regadenoson stress; for example a mean stress-MBF of approximately 0.9 ml/g/min was reported in ischemic territory while MBF remote territory in CAD patients and in non-CAD patients was approximately 2.3–2.4 ml/g/min (8). Regardless, normal values and relevant cut-offs for QP need to be clarified for each technique, consequently in our analysis we did not stratify the MBF findings by a cut-off. Moreover, this approach can be combined with rest perfusion to quantify the myocardial perfusion reserve, which has been reported to be an independent prognostic marker from stress MBF when using adenosine (34). However, we did not perform rest perfusion in our study as it is not incorporated into the local stress imaging clinical protocol. This could be investigated by integrating a rest perfusion scan before stress perfusion in further studies in which scan time can be extended to include rest perfusion. Importantly, quantitative rest perfusion after a stress perfusion using regadenoson, which was used in our study, will need further validation due to its much-longer half-life than adenosine (39).

Limitations

The used post-processing technique quantified a single transmural value per segment, and did not quantify regions of interests, sub-endocardial values or transmural gradients, which may provide more differentiated picture of the hypoperfusion (36, 41). Similarly with ECV, small regions of fibrosis within a myocardial segment can be overlooked by numerical-only analysis if the remainder of the voxels in the segment are overall normal. This could explain segments that have LGE enhancement but the averaged ECV(%) is <30%. Since both QP and ECV postprocessing methods output numerical findings and visual maps, a combination of quantitative and qualitative assessment of parametric maps may improve classification further. As this study did not collect outcome measures, it is also unclear if the MBF results are related to cardiovascular events. Nevertheless, early reports already demonstrate QP has prognostic value for major adverse cardiovascular events (34, 42). We did not acquire invasive measures of CAD, but this protocol has been externally validated to macrovascular disease measurements (10). This comparison between imaging and

invasive measures will need to be investigated further, as the goal of our study was rather to analyze the overall prevalence of hypoperfusion in a patient cohort undergoing diagnostic stress imaging in a non-tertiary institute and to investigate the impact of colocalized myocardial features on MBF.

Clinical relevance

We observed in patients referred for a clinical stress-CMR exam to test for inducible ischaemia, that post-hoc quantitative analysis detected hypoperfusion and diffuse fibrosis in myocardium beyond territories categorized as abnormal by traditional visual evaluation. Incorporating quantitative analysis into clinical work may help explain the symptoms that led to a referral for ischemic stress testing in the first place. This could be especially useful to patients who present with signs of ischemia without the traditional patterns of sub-endocardial or transmural FPP deficits and LGE. This includes investigation of pathologies such as microvascular disease, myocardial infarction with non-obstructive coronary arteries, hypertrophy among others. Use of traditional stress FPP has been shown to be a cost-effective measure by helping derive a suitable treatment plan (42, 43), and future studies can investigate if this remains true for QP analysis. Finally, the CMR studies were performed in a smaller regional hospital, demonstrating that upon further validation post-processing software and dual-bolus techniques allows imaging sites without access to specialized sequences to perform quantitative analysis, potentially facilitating future access to QP to smaller sites.

Conclusion

Quantitative perfusion image acquisition is feasible in a clinical setting and post-processing techniques can quantify pixel-wise myocardial blood flow using product perfusion sequences. Applying QP techniques, it was determined that MBF during pharmacological vasodilation was reduced in some patients independent of conventional visual FPP classification. Moreover, it was shown that ECV as a quantitative measure of diffuse fibrosis is independently associated with reduced MBF beyond focal scar on LGE images, while patient age and myocardial wall thickness are also independent contributors to hypoperfusion. Multi-parametric quantitative analysis may refine the work-up of the etiology of myocardial ischemia in patients referred for clinical CMR stress testing in the future and provide a deeper insight into ischemic heart disease.

Data availability statement

The raw data supporting the conclusions of this article will be made available by the authors, without undue reservation.

Ethics statement

The studies involving humans were approved by Ethics board of the Canton of Bern, Switzerland (2021_00139). The studies were conducted in accordance with the local legislation and institutional requirements. The participants provided their written informed consent to participate in this study.

Author contributions

JW: Data curation, Formal Analysis, Investigation, Visualization, Writing – original draft, Writing – review & editing. CH: Conceptualization, Data curation, Formal Analysis, Investigation, Project administration, Resources, Software, Supervision, Writing – review & editing. SO: Data curation, Formal Analysis, Investigation, Writing – review & editing. TK: Conceptualization, Data curation, Formal Analysis, Investigation, Project administration, Supervision, Writing – review & editing. ZS-F: Data curation, Formal Analysis, Investigation, Supervision, Writing – review & editing. RZ: Data curation, Formal Analysis, Investigation, Supervision, Writing – review & editing. DG: Conceptualization, Formal Analysis, Funding acquisition, Investigation, Methodology, Project administration, Software, Supervision, Visualization, Writing – original draft, Writing – review & editing. KF: Conceptualization, Formal Analysis, Funding acquisition, Investigation, Methodology, Project administration, Software, Supervision, Visualization, Writing – original draft, Writing – review & editing.

Funding

The author(s) declare financial support was received for the research, authorship, and/or publication of this article.

Funding is provided by the Bern University Hospital Department of Anesthesiology and Pain Medicine scientific funds (FIFK-22).

References

- Kramer CM, Barkhausen J, Bucciarelli-Ducci C, Flamm SD, Kim RJ, Nagel E. Standardized cardiovascular magnetic resonance imaging (CMR) protocols: 2020 update. *J Cardiovasc Magn Reson.* (2020) 22(1):17. doi: 10.1186/s12968-020-00607-1
- Steel K, Broderick R, Gandla V, Larose E, Resnic F, Jerosch-Herold M, et al. Complementary prognostic values of stress myocardial perfusion and late gadolinium enhancement imaging by cardiac magnetic resonance in patients with known or suspected coronary artery disease. *Circulation.* (2009) 120(14):1390–400. doi: 10.1161/CIRCULATIONAHA.108.812503
- de Ravenstein CdM, Bouzin C, Lazam S, Boulif J, Amzulescu M, Melchior J, et al. Histological validation of measurement of diffuse interstitial myocardial fibrosis by myocardial extravascular volume fraction from modified look-locker imaging (MOLLI) T1 mapping at 3T. *J Cardiovasc Magn Reson.* (2015) 17(1):48. doi: 10.1186/s12968-015-0150-0
- Kotecha T, Martinez-Naharro A, Boldrini M, Knight D, Hawkins P, Kalra S, et al. Automated pixel-wise quantitative myocardial perfusion mapping by CMR to detect obstructive coronary artery disease and coronary microvascular dysfunction: validation against invasive coronary physiology. *JACC Cardiovasc Imaging.* (2019) 12(10):1958–69. doi: 10.1016/j.jcmg.2018.12.022
- Villa ADM, Corsinovi L, Ntalas I, Milidonis X, Scannell C, Di Giovine G, et al. Importance of operator training and rest perfusion on the diagnostic accuracy of

Acknowledgments

This study was possible with the excellent work of the Radiology MR imaging technicians at the Hospital Centre of Biel.

Conflict of interest

The authors declare that the research was conducted in the absence of any commercial or financial relationships that could be construed as a potential conflict of interest.

Publisher's note

All claims expressed in this article are solely those of the authors and do not necessarily represent those of their affiliated organizations, or those of the publisher, the editors and the reviewers. Any product that may be evaluated in this article, or claim that may be made by its manufacturer, is not guaranteed or endorsed by the publisher.

Supplementary material

The Supplementary Material for this article can be found online at: <https://www.frontiersin.org/articles/10.3389/fcvm.2023.1260156/full#supplementary-material>

SUPPLEMENTARY VIDEO S1

Quantitative perfusion analysis. Example of steps required for the post-processing. In this study only stress perfusion was acquired. Processing performed using a 2018 MacBook Pro with a 2.7 GHz Quad-Core Intel Core i7 processor.

- stress perfusion cardiovascular magnetic resonance. *J Cardiovasc Magn Reson.* (2018) 20:74. doi: 10.1186/s12968-018-0493-4
- Mordini FE, Haddad T, Hsu LY, Kellman P, Lowrey TB, Aletras AH, et al. Diagnostic accuracy of stress perfusion CMR in comparison with quantitative coronary angiography: fully quantitative, semiquantitative, and qualitative assessment. *JACC Cardiovasc Imaging.* (2014) 7(1):14–22. doi: 10.1016/j.jcmg.2013.08.014
- Bradley AJ, Groves DW, Benovoy M, Yang SK, Kozlov S, Taylor JL, et al. Three automated quantitative cardiac magnetic resonance perfusion analyses versus invasive fractional flow reserve in swine. *JACC Cardiovasc Imaging.* (2021) 14(9):1871–3. doi: 10.1016/j.jcmg.2021.03.013
- Hsu LY, Jacobs M, Benovoy M, Ta AD, Conn HM, Winkler S, et al. Diagnostic performance of fully automated pixel-wise quantitative myocardial perfusion imaging by cardiovascular magnetic resonance. *JACC Cardiovasc Imaging.* (2018) 11(5):697–707. doi: 10.1016/j.jcmg.2018.01.005
- Jacobs M, Benovoy M, Chang LC, Corcoran D, Berry C, Arai AE, et al. Automated segmental analysis of fully quantitative myocardial blood flow maps by first-pass perfusion cardiovascular magnetic resonance. *IEEE Access Pract Innov Open Solut.* (2021) 9:52796–811. doi: 10.1109/access.2021.3070320
- Zhao SH, Guo WF, Yao ZF, Yang S, Yun H, Chen YY, et al. Fully automated pixel-wise quantitative CMR-myocardial perfusion with CMR-coronary

- angiography to detect hemodynamically significant coronary artery disease. *Eur Radiol.* (2023). doi: 10.1007/s00330-023-09689-8. [Online ahead of print]
11. Utz W, Greiser A, Niendorf T, Dietz R, Schulz-Menger J. Single- or dual-bolus approach for the assessment of myocardial perfusion reserve in quantitative MR perfusion imaging. *Magn Reson Med.* (2008) 59(6):1373–7. doi: 10.1002/mrm.21611
 12. Treibel TA, Fontana M, Maestrini V, Castelletti S, Rosmini S, Simpson J, et al. Automatic measurement of the myocardial interstitium. *JACC Cardiovasc Imaging.* (2016) 9(1):54–63. doi: 10.1016/j.jcmg.2015.11.008
 13. Kotecha T, Chacko L, Chehab O, O'Reilly N, Martinez-Naharro A, Lazari J, et al. Assessment of multivessel coronary artery disease using cardiovascular magnetic resonance pixelwise quantitative perfusion mapping. *JACC Cardiovasc Imaging.* (2020) 13(12):2546–57. doi: 10.1016/j.jcmg.2020.06.041
 14. Camaioni C, Knott KD, Augusto JB, Seraphim A, Rosmini S, Ricci F, et al. In-line perfusion mapping provides insights into the disease mechanism in hypertrophic cardiomyopathy. *Heart.* (2020) 106(11):824–9. doi: 10.1136/heartjnl-2019-315848
 15. Spicher B, Fischer K, Zimmerli ZA, Yamaji K, Ueki Y, Bertschinger CN, et al. Combined analysis of myocardial deformation and oxygenation detects inducible ischemia unmasked by breathing maneuvers in chronic coronary syndrome. *Front Cardiovasc Med.* (2022) 9:e800720. doi: 10.3389/fcvm.2022.800720
 16. Palumbo P, Cannizzaro E, Di Cesare A, Bruno F, Arrigoni F, Splendiani A, et al. Stress perfusion cardiac magnetic resonance in long-standing non-infarcted chronic coronary syndrome with preserved systolic function. *Diagnostics.* (2022) 12(4):786. doi: 10.3390/diagnostics12040786
 17. Guensch DP, Fischer K, Yamaji K, Luescher S, Ueki Y, Jung B, et al. Effect of hyperoxia on myocardial oxygenation and function in patients with stable multivessel coronary artery disease. *J Am Heart Assoc.* (2020) 9(5):e014739. doi: 10.1161/JAHA.119.014739
 18. Heusch G, Libby P, Gersh B, Yellon D, Böhm M, Lopaschuk G, et al. Cardiovascular remodelling in coronary artery disease and heart failure. *Lancet.* (2014) 383(9932):1933–43. doi: 10.1016/S0140-6736(14)60107-0
 19. Cowling RT, Kupsky D, Kahn AM, Daniels LB, Greenberg BH. Mechanisms of cardiac collagen deposition in experimental models and human disease. *Transl Res.* (2019) 209:138–55. doi: 10.1016/j.trsl.2019.03.004
 20. Haaf P, Garg P, Messroghli DR, Broadbent DA, Greenwood JP, Plein S. Cardiac T1 mapping and extracellular volume (ECV) in clinical practice: a comprehensive review. *J Cardiovasc Magn Reson.* (2016) 18(1):89. doi: 10.1186/s12968-016-0308-4
 21. Schelbert EB, Sabbah HN, Butler J, Gheorghide M. Employing extracellular volume cardiovascular magnetic resonance measures of myocardial fibrosis to foster novel therapeutics. *Circ Cardiovasc Imaging.* (2017) 10(6):e005619. doi: 10.1161/CIRCIMAGING.116.005619
 22. Sabbah HN, Sharov VG, Lesch M, Goldstein S. Progression of heart failure: a role for interstitial fibrosis. *Mol Cell Biochem.* (1995) 147(1–2):29–34. doi: 10.1007/BF00944780
 23. Guensch DP, Kuganathan S, Utz CD, Neuenschwander MD, Grob L, Becker P, et al. Analysis of bi-atrial function using CMR feature tracking and long-axis shortening approaches in patients with diastolic dysfunction and atrial fibrillation. *Eur Radiol.* (2023). doi: 10.1007/s00330-023-09663-4. [Online ahead of print]
 24. Selma F, M, Saad H, Sultan A. M, William D. E, Joseph J. M, Margaret M R. Coronary microvascular rarefaction and myocardial fibrosis in heart failure with preserved ejection fraction. *Circulation.* (2015) 131(6):550–9. doi: 10.1161/CIRCULATIONAHA.114.009625
 25. Taqueti VR, Di Carli MF. Coronary microvascular disease pathogenic mechanisms and therapeutic options: JACC state-of-the-art review. *J Am Coll Cardiol.* (2018) 72(21):2625–41. doi: 10.1016/j.jacc.2018.09.042
 26. Saeed M, Wendland MF, Watzinger N, Akbari H, Higgins CB. MR Contrast media for myocardial viability, microvascular integrity and perfusion. *Eur J Radiol.* (2000) 34(3):179–95. doi: 10.1016/S0720-048X(00)00198-4
 27. Ugander M, Bagi PS, Oki AJ, Chen B, Hsu LY, Aletras AH, et al. Myocardial edema as detected by pre-contrast T1 and T2 CMR delineates area at risk associated with acute myocardial infarction. *JACC Cardiovasc Imaging.* (2012) 5(6):596–603. doi: 10.1016/j.jcmg.2012.01.016
 28. Guensch DP, Michel MC, Huettenmoser SP, Jung B, Gulac P, Segiser A, et al. The blood oxygen level dependent (BOLD) effect of in-vitro myoglobin and hemoglobin. *Sci Rep.* (2021) 11(1):11464. doi: 10.1038/s41598-021-90908-x
 29. Pedersen SF, Thrysøe SA, Robich MP, Paaske WP, Ringgaard S, Bøtker HE, et al. Assessment of intramyocardial hemorrhage by T1-weighted cardiovascular magnetic resonance in reperfused acute myocardial infarction. *J Cardiovasc Magn Reson.* (2012) 14(1):59. doi: 10.1186/1532-429X-14-59
 30. Jablonowski R, Engblom H, Kanski M, Nordlund D, Koul S, van der PJ, et al. Contrast-enhanced CMR overestimates early myocardial infarct size. *JACC Cardiovasc Imaging.* (2015) 8(12):1379–89. doi: 10.1016/j.jcmg.2015.08.015
 31. Petersen SE, Jerosch-Herold M, Hudsmith LE, Robson MD, Francis JM, Doll HA, et al. Evidence for microvascular dysfunction in hypertrophic cardiomyopathy new insights from multiparametric magnetic resonance imaging. *Circulation.* (2007) 115(18):2418–25. doi: 10.1161/CIRCULATIONAHA.106.657023
 32. Knott KD, Augusto JB, Nordin S, Kozor R, Camaioni C, Xue H, et al. Quantitative myocardial perfusion in fabry disease. *Circ Cardiovasc Imaging.* (2019) 12(7):e008872. doi: 10.1161/CIRCIMAGING.119.008872
 33. Fischer K, Guensch DP, Jung B, King I, von Tengg-Kobligk H, Giannetti N, et al. Insights into myocardial oxygenation and cardiovascular magnetic resonance tissue biomarkers in heart failure with preserved ejection fraction. *Circ Heart Fail.* (2022) 15(4):e008903. doi: 10.1161/CIRCHEARTFAILURE.121.008903
 34. Knott KD, Seraphim A, Augusto JB, Xue H, Chacko L, Aung N, et al. The prognostic significance of quantitative myocardial perfusion. *Circulation.* (2020) 141(16):1282–91. doi: 10.1161/CIRCULATIONAHA.119.044666
 35. Kellman P, Hansen MS, NIELLES-Vallespin S, Nickander J, Themudo R, Ugander M, et al. Myocardial perfusion cardiovascular magnetic resonance: optimized dual sequence and reconstruction for quantification. *J Cardiovasc Magn Reson.* (2017) 19(1):43. doi: 10.1186/s12968-017-0355-5
 36. Knott KD, Camaioni C, Ramasamy A, Augusto JA, Bhuvana AN, Xue H, et al. Quantitative myocardial perfusion in coronary artery disease: a perfusion mapping study. *J Magn Reson Imaging.* (2019) 50(3):756–62. doi: 10.1002/jmri.26668
 37. Ta AD, Hsu LY, Conn HM, Winkler S, Greve AM, Shanbhag SM, et al. Fully quantitative pixel-wise analysis of cardiovascular magnetic resonance perfusion improves discrimination of dark rim artifact from perfusion defects associated with epicardial coronary stenosis. *J Cardiovasc Magn Reson.* (2018) 20:16. doi: 10.1186/s12968-018-0436-0
 38. Zorach B, Shaw PW, Bourque J, Kuruvilla S, Balfour PC, Yang Y, et al. Quantitative cardiovascular magnetic resonance perfusion imaging identifies reduced flow reserve in microvascular coronary artery disease. *J Cardiovasc Magn Reson.* (2018) 20:14. doi: 10.1186/s12968-018-0435-1
 39. Bhavne NM, Freed BH, Yodwut C, Kolanczyk D, Dill K, Lang RM, et al. Considerations when measuring myocardial perfusion reserve by cardiovascular magnetic resonance using regadenoson. *J Cardiovasc Magn Reson Off J Soc Cardiovasc Magn Reson.* (2012) 14(1):89. doi: 10.1186/1532-429X-14-89
 40. Sammut E, Zarinabad N, Wesolowski R, Morton G, Chen Z, Sohal M, et al. Feasibility of high-resolution quantitative perfusion analysis in patients with heart failure. *J Cardiovasc Magn Reson.* (2015) 17(1):13. doi: 10.1186/s12968-015-0124-2
 41. Sammut EC, Villa ADM, Giovine GD, Dancy L, Bosio F, Gibbs T, et al. Prognostic value of quantitative stress perfusion cardiac magnetic resonance. *JACC Cardiovasc Imaging.* (2018) 11(5):686–94. doi: 10.1016/j.jcmg.2017.07.022
 42. Hendel RC, Friedrich MG, Jeanette S-M, Zemmrich C, Bengel F, Berman DS, et al. CMR first-pass perfusion for suspected inducible myocardial ischemia. *JACC Cardiovasc Imaging.* (2016) 9(11):1338–48. doi: 10.1016/j.jcmg.2016.09.010
 43. Boldt J, Leber AW, Bonaventura K, Sohns C, Stula M, Huppertz A, et al. Cost-effectiveness of cardiovascular magnetic resonance and single-photon emission computed tomography for diagnosis of coronary artery disease in Germany. *J Cardiovasc Magn Reson.* (2013) 15(1):30. doi: 10.1186/1532-429X-15-30